Structural effects on the magnetic character of yttrium–iron–garnet nanoparticles dispersed in glass composites

Susamu Taketomi,[a] Alexander J. Shapiro, and Robert D. Shull
National Institute of Standards and Technology, Gaithersburg, Maryland 20899-8552

(Presented on 13 November 2002)

By absorbing amorphous yttrium–iron–garnet nanoparticles into nanometer pores of the sponge-like structure of porous silica glass [controlled pore glass (CPG)] followed by heat treatment, we obtained dispersed-nanocrystal/glass composites. We prepared samples using different extremal heat treatments: low temperature long calcination (700 °C, 2 h) and high temperature short calcination (1000 °C, 0.1 h). From the difference between the secondary electron image in a field emission scanning electron microscope (FESEM) and the backscattered electron image of the same sample surface area, it is concluded that the nanoparticles were imbedded on and just beneath the surface of the CPG granules. This was confirmed by a cross-sectional backscattered electron image of the sample in the FESEM. In this image nanoparticles of 20–40 nm were monodispersed in a 2 μm thick shell of fused glass and, inside this shell, the inner core of CPG granules preserved their sponge-like structure and contained no nanoparticles. Powder x-ray diffraction revealed that the synthesized nanoparticles were dominantly ϵ-Fe_2O_3, however, many small diffraction peaks consistent with those of $Fe_5Y_3O_{12}$ and $FeYO_3$, were also observed. The magnetization hysteresis loop curves revealed that the high temperature heat-treated samples were paramagnetic, whereas the low-temperature heat-treated sample was a mixture of a small amount of ferro- or ferrimagnetic material with a majority being paramagnetic material. [DOI: 10.1063/1.1555900]

I. INTRODUCTION

Fine magnetic particles have been shown to possess properties different from their bulk counterparts, partly as a consequence of having no magnetic domains if their size is very fine and partly because of the appearance of quantum size effects for small particle sizes. Because processing can affect both these characteristics, it is of interest to understand the synthesis as well as the type of fine particle mixtures that can be prepared and their connection to the magnetic properties they possess. For very fine particles their mutual interaction can also be studied without magnetic domain effects. Fine magnetic particles are also of interest due to their potential application as media in high density magnetic information storage.

We prepared a dispersion of yttrium–iron oxide nanoparticles in controlled pore glass (CPG) using a technique described earlier.[1] The CPG is a sponge-like-structure that contains a network of pores with diameters that are tens of nanometers.[2,3] After preparing a colloidal solution of amorphous yttrium–iron–garnet (YIG) nanoparticles by an alkoxide method,[4] we infiltrated that solution through the CPG pores and into the sponge-like structure of the glass and then evaporated the solvent. During infiltration, the well controlled nanometer-sized pores of the glass acted as a filter, screening out all amorphous YIG particles larger than the pore diameter. We call this material the ''sample predecessor'' in this article. Finally we heat treated this sample predecessor, and the amorphous YIG nanoparticles crystallized in the pores and formed yttrium–iron oxide nanocrystals. Simultaneously, the sponge-like structure of the pores fused together and the nanocrystal-dispersed glass composite was created. X-ray diffraction data and transmission electron microscopy observations have shown that, depending on the thermal treatment, various yttrium–iron oxides, including YIG, formed inside the CPG.[1] In addition, their magnetic properties were correlated with the crystalline phases identified.[5] In this article we report high resolution field emission scanning electron microscopy (FESEM) observations of the surface and cross section of a newly prepared sample that show the shapes and locations of the nanocrystals, and correlate these with further x-ray diffraction measurements and magnetization data.

II. SAMPLE PREPARATION

The sample predecessor used in the present study consisted of a powder with granule diameters of approximately 50 μm. An earlier study revealed that it was necessary to heat the sample predecessor at temperatures at least as hot as 700 °C in order to crystallize the nanoparticles in the YIG structure.[4] However, if the sample predecessor was heat treated at high temperature for too long a time, the YIG nanoparticles reacted with the surrounding silica and formed many different iron silicate or yttrium silicate compounds.[1] Therefore, in order to obtain crystalline YIG nanoparticles it is necessary to heat treat the sample predecessors for only a short time at high temperature. The heat treatments were performed with the sample predecessor in a crucible, which

[a]Permanent address: Matsumoto Yushi-Seiyaku Co. Ltd., Yao, Osaka 581-0075 Japan; electronic mail: taketomi@nist.gov

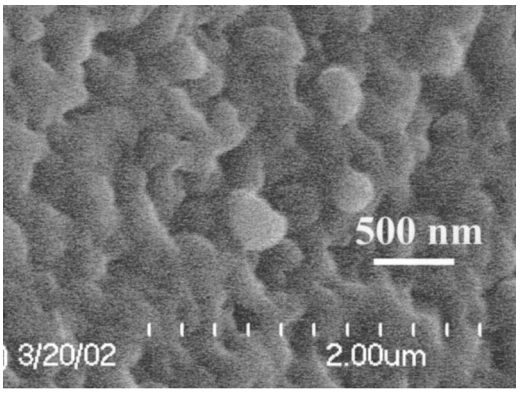

(a)

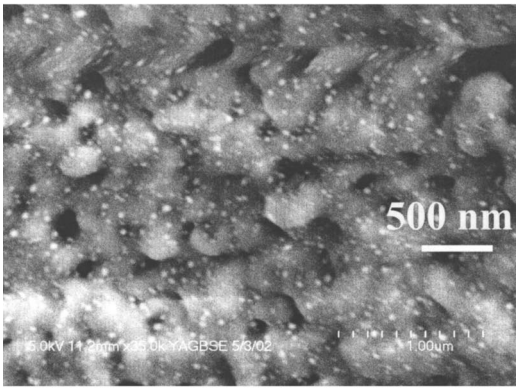

(b)

FIG. 1. Field emission scanning electron micrograph of sample A: (a) secondary electron image; (b) backscattered electron image.

was placed inside an electric furnace at constant temperature, $T_0(°C)$ for t_0 (hours) and air cooled. Measurements of a control sample showed that the sample's temperature reached the furnace temperature a few minutes after it was placed in the furnace. Three samples, A, B, and C, were prepared using sample predecessor CPGs with different pore sizes, d_0 (nm). The set of values (T_0, t_0, d_0) for samples A, B, and C are 1000, 0.1, and 100, 1000, 0.1, and 49, and 700, 2, and 200, respectively.

III. RESULTS

A. FESEM observation

Figures 1(a) and 1(b) are the secondary electron image and the backscattered electron image, respectively, of the same region of the surface of sample A. The acceleration voltage was 5 kV for both images. In Fig. 1(a), it is apparent that the CPG did not completely fuse; it consists of large chunks of fused glass connected to each other. No nanoparticles are observed in this image. On the contrary, in Fig. 1(b) many nanoparticles, or white spots, are observed dispersed on the surface of the completely fused CPG. Generally speaking, the white contrast in the secondary electron image shows the relative closeness of that region on the object's surface compared to neighboring areas. On the other hand, white contrast in a backscattered electron image shows not only the unevenness of the surface but also the difference in

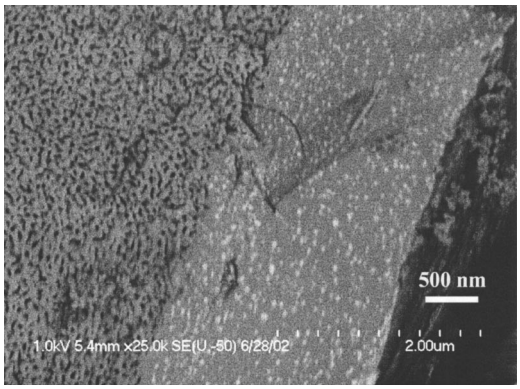

FIG. 2. Backscattered electron image of sample B's cracked cross section.

elemental composition. In the present case, the area where iron and yttrium elements are rich shows white contrast and black contrast, indicating areas where there is a lack of these elements. Consequently, Fig. 1(b) shows the ''white spot'' nanoparticles consist of Fe and Y, and are hence the YIG particles.

It was found that sample B was very brittle, and if pressed between steel plates by hand, its granules easily cracked. Figure 2 shows the backscattered electron image of a freshly cut cross section of this sample. The ≈ 2 μm wide layer on the right is the fused silica phase containing the dispersed nanoparticles (white spots), and the inner core phase of the nonfused pure CPG is shown on the left. Note the particles did not cluster but were independently dispersed with sizes ranging from 20 to 40 nm. Also note the particles are surprisingly nonspherical. On the other hand, the inner CPG preserved its initial sponge-like structure and no nanoparticles were found in this region. It is concluded that the nanoparticles acted as catalysts and fused with the CPG. The average particle density was $110/\mu m^2$, but became greater the nearer it was to the surface. The right edge of the image is the surface of the granule. The deeper inner surface area was also observed due to the long focal depth of the FESEM.

B. X-ray diffraction

Figure 3 shows the x-ray diffraction intensity (x-ray wavelength $\lambda = 0.154$ nm) as a function of diffraction angle 2θ for the three samples, A, B, and C, respectively. The nanoparticles' volume fraction was so small in these samples compared to in the CPG matrix that the diffraction intensity from the nanoparticles was very weak. To overcome this, we used rather large x-ray beam slits to increase the beam intensity and measured the x-ray intensity for 60 s each diffraction angle so that the signal to noise (S/N) ratio could be increased. The angle interval was 0.1°. Consequently, the counting statistics were good, and the many weak peaks observed in the diffraction intensity curve did not constitute noise in the data, but are instead significant. In sample C, the CPG matrix was crystallized to cristobalite, whereas it remained amorphous in the other two samples. The enhancement around $2\theta = 22°$ was a halo from the glass. Several

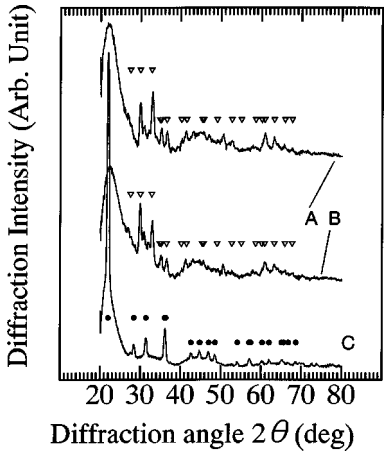

FIG. 3. Powder x-ray diffraction: ● cristobalite (39-1425); ▽ ϵ-Fe_2O_3(16-0653). The numbers are identifying numbers of the powder data file of the Joint Committee on Powder Diffraction Standards.

dominant peaks in samples A and B coincide with the diffraction lines of ϵ-Fe_2O_3. So far, only cristobalite has been definitively identified. However, if we take the many weak diffraction peaks into account there is the possible existence of $Fe_5Y_3O_{12}$ and $FeYO_3$.

C. Magnetization curves

The magnetic hysteresis loop of each sample measured by a vibrating sample magnetometer (VSM) is shown in Fig. 4. These data were obtained at room temperature as follows. After magnetically saturating the sample by applying a 750 kA/m magnetic field, H, the sample magnetization, M, was measured while the field was sequentially decreased to -750 kA/m and then increased back to $+750$ kA/m. In this article we use SI units: $\boldsymbol{B}=\mu_0(\boldsymbol{H}+\boldsymbol{M})$, where $\boldsymbol{B}$ is the magnetic flux density and μ_0 is magnetic permittivity in vacuum. However, M in Fig. 4 is not the magnetization per unit volume, but is instead the magnetization per unit mass of the composite ($A\,m^2/kg$). Samples A and B are paramagnetic. Since sample A's initial CPG pore size was greater than that of sample B's, the mass of the absorbed nanoparticles in sample A's predecessor was larger than that in sample B's predecessor. Consequently, the magnetic susceptibility (indicated by the slope of the $M-H$ curve) of sample A is larger than that of sample B. ϵ-Fe_2O_3 was reported to be ferrimagnetic.[6,7] However, in this study samples A and B, which may possess this unusual phase, only show paramagnetic behavior. This may be that, due to smallness of the ϵ-Fe_2O_3 nanocrystals in these samples, the highly dispersed nature of these particles would make the material superparamagnetic. Consequently, if only the linear low field regime of the magnetization curve is observed, the material may appear to be paramagnetic despite the ferromagnetic nature of the nanocrystals. Partially on the basis of the large magnetic susceptibility of sample C, it is concluded to be a mixture of a small amount of ferri- or ferromagnetic material with a majority being paramagnetic material. This conclusion is also consistent with the small residual magnetization ($<0.07\ A\,m^2/kg$) that was also found for this sample.

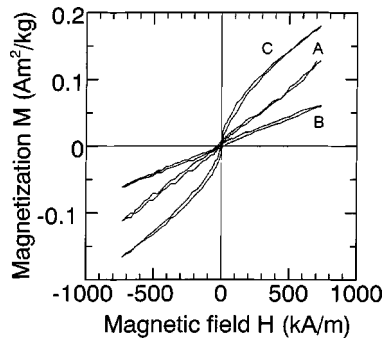

FIG. 4. Magnetization vs applied magnetic field hysteresis loops for samples A, B, and C measured at 27 °C.

IV. CONCLUSION

By absorbing amorphous yttrium–iron–garnet nanoparticles into nanometer pores of the sponge-like structure of porous silica glass (controlled pore glass) followed by heat treatment, we obtained dispersed-nanocrystal/glass composites. We prepared samples using different heat treatments: low temperature, long calcination (700 °C, 2 h) and high temperature, short calcination (1000 °C, 0.1 h). We made FESEM observations, x-ray diffraction identifications, and magnetic measurements of these samples. No nanoparticles were observed on the sample surface by secondary electron imaging in the FESEM whereas they were detected by backscattered electron imaging. This was confirmed by the cross-sectional backscattered electron image in the FESEM image of the sample. In this latter image, the nanoparticles were monodispersed in a 2 μm thick shell of fused glass and were 20–40 nm. Inside this shell, the inner core of CPG granules preserved their sponge-like structure and contained no nanoparticles. Powder x-ray diffraction revealed that the synthesized nanoparticles were predominantly ϵ-Fe_2O_3 for the high-temperature heat-treated samples. No identification of nanoparticles in the low-temperature heat-treated sample was made. However many small diffraction peaks consistent with those of $Fe_5Y_3O_{12}$ and $FeYO_3$ were observed in all the samples. The magnetization hysteresis loop curves revealed that the high temperature heat-treated samples were paramagnetic. However these samples might be superparamagnetic due to the nanometer-size scale of ϵ-Fe_2O_3 particles. It was also revealed that the low-temperature heat-treated sample was a mixture of a small amount of ferro- or ferrimagnetic material with a majority being paramagnetic material.

[1] S. Taketomi, C. M. Sorensen, and K. J. Klabunde, J. Magn. Magn. Mater. **222**, 54 (2000).
[2] W. Haller, J. Chem. Phys. **42**, 686 (1965).
[3] W. Haller, Nature (London) **206**, 693 (1965).
[4] S. Taketomi, K. Kawasaki, Y. Ozaki, S. Yuasa, Y. Otani, and H. Miyajima, J. Am. Ceram. Soc. **77**, 1787 (1994).
[5] S. Taketomi and R. D. Shull, J. Appl. Phys. **91**, 8468 (2002).
[6] R. Von Schrader and G. Büttner, Z. Anorg. Allg. Chem. **320**, 220 (1963).
[7] E. Tronc, C. Chaneac, and J. P. Jolovet, J. Solid State Chem. **139**, 93 (1998).